A partially coupled ocean–atmosphere model for retrieval of water-leaving radiance from SeaWiFS in coastal waters

Article · May 2003

CITATIONS
186

READS
377

5 authors, including:

Richard P Stumpf
National Oceanic and Atmospheric Administration
135 PUBLICATIONS **4,709** CITATIONS

SEE PROFILE

Robert Arnone
University of Southern Mississippi
277 PUBLICATIONS **5,582** CITATIONS

SEE PROFILE

Varis Ransibrahmanakul
27 PUBLICATIONS **715** CITATIONS

SEE PROFILE

NASA/TM–2003–206892, Vol. 22

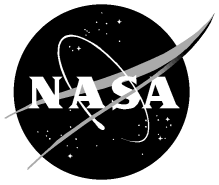

SeaWiFS Postlaunch Technical Report Series

Stanford B. Hooker and Elaine R. Firestone, Editors

Volume 22, Algorithm Updates for the Fourth SeaWiFS Data Reprocessing

Frederick S. Patt, Robert A. Barnes, Robert E. Eplee, Jr., Bryan A. Franz, Wayne D. Robinson, Gene Carl Feldman, Sean W. Bailey, Joel Gales, P. Jeremy Werdell, Menghua Wang, Robert Frouin, Richard P. Stumpf, Robert A. Arnone, Richard W. Gould, Jr., Paul M. Martinolich, Varis Ransibrahmanakul, John E. O'Reilly, and James A. Yoder

National Aeronautics and
Space Administration

Goddard Space Flight Center
Greenbelt, Maryland 20771

May 2003

The NASA STI Program Office ... in Profile

Since its founding, NASA has been dedicated to the advancement of aeronautics and space science. The NASA Scientific and Technical Information (STI) Program Office plays a key part in helping NASA maintain this important role.

The NASA STI Program Office is operated by Langley Research Center, the lead center for NASA's scientific and technical information. The NASA STI Program Office provides access to the NASA STI Database, the largest collection of aeronautical and space science STI in the world. The Program Office is also NASA's institutional mechanism for disseminating the results of its research and development activities. These results are published by NASA in the NASA STI Report Series, which includes the following report types:

- TECHNICAL PUBLICATION. Reports of completed research or a major significant phase of research that present the results of NASA programs and include extensive data or theoretical analysis. Includes compilations of significant scientific and technical data and information deemed to be of continuing reference value. NASA's counterpart of peer-reviewed formal professional papers but has less stringent limitations on manuscript length and extent of graphic presentations.

- TECHNICAL MEMORANDUM. Scientific and technical findings that are preliminary or of specialized interest, e.g., quick release reports, working papers, and bibliographies that contain minimal annotation. Does not contain extensive analysis.

- CONTRACTOR REPORT. Scientific and technical findings by NASA-sponsored contractors and grantees.

- CONFERENCE PUBLICATION. Collected papers from scientific and technical conferences, symposia, seminars, or other meetings sponsored or cosponsored by NASA.

- SPECIAL PUBLICATION. Scientific, technical, or historical information from NASA programs, projects, and mission, often concerned with subjects having substantial public interest.

- TECHNICAL TRANSLATION. English-language translations of foreign scientific and technical material pertinent to NASA's mission.

Specialized services that complement the STI Program Office's diverse offerings include creating custom thesauri, building customized databases, organizing and publishing research results... even providing videos.

For more information about the NASA STI Program Office, see the following:

- Access the NASA SIT Program Home Page at http://www.sti.nasa.gov/STI-homepage.html

- E-mail your question via the Internet to help@sti.nasa.gov

- Fax your question to the NASA Access Help Desk at (301) 621-0134

- Write to:
  NASA Access Help Desk
  NASA Center for Aerospace Information
  7121 Standard Drive
  Hanover, MD 21076-1320

NASA/TM–2003–206892, Vol. 22

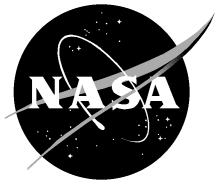

SeaWiFS Postlaunch Technical Report Series

Stanford B. Hooker, Editor
NASA Goddard Space Flight Center, Greenbelt, Maryland

Elaine R. Firestone, Senior Scientific Technical Editor
Science Applications International Corporation, Beltsville, Maryland

Volume 22, Algorithm Updates for the Fourth SeaWiFS Data Reprocessing

Frederick S. Patt, Robert A. Barnes, Robert E. Eplee, Jr., Bryan A. Franz, and Wayne D. Robinson
Science Applications International Corporation, Beltsville, Maryland

Gene Carl Feldman
NASA Goddard Space Flight Center, Greenbelt, Maryland

Sean W. Bailey and Joel Gales
Futuretech Corporation, Greenbelt, Maryland

P. Jeremy Werdell
Science Systems and Applications, Incorporated, Lanham, Maryland

Menghua Wang
University of Maryland, Baltimore County, Baltimore, Maryland

Robert Frouin
Scripps Institution of Oceanography, La Jolla, California

Richard P. Stumpf
NOAA Center for Coastal Monitoring and Assessment, Silver Spring, Maryland

Robert A. Arnone, Richard W. Gould, Jr., and Paul M. Martinolich
Naval Research Lab, Stennis, Mississippi

Varis Ransibrahmanakul
SPS Technologies, Silver Spring, Maryland

John E. O'Reilly
NOAA National Marine Fisheries Service, Narragansett, Rhode Island

James A. Yoder
University of Rhode Island, Narragansett, Rhode Island

May 2003

ISSN 1522-8789

Available from:

NASA Center for AeroSpace Information
7121 Standard Drive
Hanover, MD 21076–1320
Price Code: A17

National Technical Information Service
5285 Port Royal Road
Springfield, VA 22161
Price Code: A10

Chapter 9

A Partially Coupled Ocean–Atmosphere Model for Retrieval of Water-Leaving Radiance from SeaWiFS in Coastal Waters

Richard P. Stumpf
NOAA Center for Coastal Monitoring and Assessment
Silver Spring, Maryland

Robert A. Arnone, Richard W. Gould, Jr., and Paul M. Martinolich
Naval Research Lab
Stennis, Mississippi

Varis Ransibrahmanakul
SPS Technologies
Silver Spring, Maryland

Abstract

The global atmospheric correction algorithm for SeaWiFS tends to over correct for the atmosphere in coastal waters because of water-leaving radiance (L_W) in the NIR part of the spectrum, λ_r. This $L_W(\lambda_r)$ phenomenon occurs particularly in water with high inorganic particulate levels. An iterative solution is used to solve this problem. A bio-optical model is used to determine the NIR backscatter from the backscatter at 670 nm, and specifically addresses inorganic particulates. This solution requires compensation for absorption by chlorophyll, detrital pigments, and gelbstoff (colored dissolved organic matter). The $L_W(\lambda_r)$ is found and removed from the total radiance so that the standard atmospheric models can be applied. Chlorophyll *a* concentrations, C_a, in coastal and Case-2 waters are reduced to appropriate levels. The algorithm cannot yet correct areas where negative L_W occurs at 670 nm.

9.1 INTRODUCTION

The use of satellites to monitor the color of the ocean requires effective removal of the atmospheric signal. The methods for treating the atmosphere have depended on the high absorption of red and NIR light by water. In open ocean water where only C_a and related pigments determine the optical properties, water can be considered to absorb all light, so that the signal observed by the satellite should result entirely from the atmospheric path radiance. While the scattering due to Rayleigh, and absorption due to ozone and other gases can be treated through computation with appropriate lookup tables to address seasonal and latitudinal effects (Gordon et al. 1983 and Gordon and Wang 1994), the aerosol optical depth must be computed for each pixel.

The aerosol correction has required determination of two major factors:

1) The amount of aerosol, characterized by the optical depth; and
2) The type of aerosol, which determines the size distribution and apparent color, and is characterized by either the Ångström exponent, or ϵ.

The atmospheric correction for the Coastal Zone Color Scanner (CZCS) used a band at 665 nm (CZCS band 4) to provide a correction for the aerosol optical depth (Gordon et al. 1983), with additional assumptions about the spectra for water with negligible C_a (Gordon and Clark 1981), and calculates the ϵ value for each scene (but not each pixel). The 665 nm band is positioned where the absorption of water becomes significant (Table 9), thus, the entire radiance in the CZCS correction is presumed to originate in the atmosphere.

It was recognized immediately that water with a detectable scattering component, in particular inorganic sediment, had detectable radiance at this wavelength. Smith and Wilson (1981) proposed an iterative solution based on assumptions of the spectral relationship between 443, 550, and 670 nm. Later, Mueller (1984) proposed another so-

lution using C_a to estimate the radiance at 670 nm. In both solutions, the estimated water-leaving radiance (L_W) at 670 nm is removed from the signal, then the normalized water-leaving radiances, L_{WN}, are recalculated and the L_W values are re-estimated. When the change in L_{WN} values becomes negligible, the iteration ends. Gould and Arnone (1994) altered the approach by using estimates of the diffuse attenuation to obtain the estimated L_W, and significantly improved the usefulness of CZCS data in clearer Case-2 waters. While these are the best approaches for CZCS, these iterations are based on in-water optical properties which are limited by their dependence on consistent spectral relationships between the bands. These spectral relationships will vary with changes in the optical constituents. In addition, use of the 670 nm band for atmospheric correction can produce unpredictable results as $L_W(670)$ can also become greater than the aerosol radiance [$L_a(670)$], making the result unreliable. The iteration further depends on consistent spectral relationships between the bands. These relationships can vary owing to changes in the optical constituents.

Table 9. Water absorption at the SeaWiFS bands (Curcio and Perry 1951, Palmer and Williams 1974, Smith and Baker 1981, and Pope and Fry 1997).

Band No.	*Wavelength* [nm]	*Bandwidth* [nm]	*Absorption* [m^{-1}]
1	412	20	0.00450
2	443	20	0.00700
3	490	20	0.01500
4	510	20	0.03250
5	555	20	0.06000
6	670	20	0.43000
7	765	40	2.50000
8	865	40	4.30000

With SeaWiFS, bands for atmospheric correction were introduced in the NIR at 765 and 865 nm (Table 9). The absorption of water at these bands is sixfold and tenfold, respectively, of the absorption at 665 nm, producing negligible water-leaving radiance in most Case-1 waters. In addition, the two bands offer a means of deriving an atmospheric model that adjusts for aerosol type by determining $\epsilon(\lambda_i, \lambda_j)$ at each pixel, where ϵ relates the aerosol radiance at band λ_i to a reference band λ_j (Gordon and Wang 1994). In coastal waters having high concentrations of scattering material, water-leaving radiance can still occur in the NIR, an effect noted previously by researchers using other sensors that had NIR bands [Moore (1980), Stumpf and Tyler (1988), and Stumpf and Pennock (1989)].

The presence of water-leaving radiance in the NIR introduces two sources of error into the removal of the aerosol. First, the total aerosol is overestimated as some of the total radiance (L_t) at 865 nm derives from the water. Second, as the absorption of water changes from 765–865 nm, the selection of the appropriate atmospheric model is affected, causing an error in the extrapolation of the aerosol radiance to the shorter wavelengths. As a result, the atmospheric radiances will be overestimated at all bands with increasing severity for shorter wavelengths, even leading to negative radiances in the blue bands in coastal water. This results in severe errors, if not complete failure, of various algorithms for C_a and optical properties.

To solve this problem, iterative solutions were proposed. Land and Haigh (1996) developed a solution for SeaWiFS that involved modeling the water reflectance and atmospheric aerosol at all wavelengths to convergence. They attempted to solve simultaneously for both the ocean and atmosphere at all wavelengths. While a promising solution, this attempt puts severe demands on the accuracy of the bio-optical model.

For the Medium Resolution Imaging Spectrometer (MERIS), Moore et al. (1999) developed an iteration based on three NIR bands to estimate the NIR water radiance based on the Gordon and Wang (1994) solution. This solution is promising, but does not apply to SeaWiFS or MODIS, both of which have fewer NIR bands.

Gould et al. (1998) proposed an iteration for SeaWiFS that determined NIR scattering from 670 nm scattering, which is the basis for the scattering component presented here. The solution addressed only the absorption by water.

Ruddick et al. (2000) developed a method that solves for the aerosol radiance and L_W simultaneously in the NIR to good results in highly scattering systems in the North Sea. This method uses a single aerosol type (constant ϵ value) determined manually, which poses problems for automated processing.

Hu et al. (2000b) developed a technique to transfer the ϵ value from the nearest clear water. While potentially effective, it depends on the aerosol type remaining spatially constant in the coastal zone, potentially over hundreds of kilometers.

Siegel et al. (2000) developed an iterative technique that presumed the backscatter to covary with C_a and used the Gordon and Wang model to solve for the NIR backscatter. This model has been implemented by NASA, but is most effective in Case-1 water or in water where sediment covaries with C_a.

The information presented in this chapter is a partially coupled solution for SeaWiFS (and ultimately MODIS), where the scattering problems of atmosphere and water scattering in the NIR are coupled. A variation on this model was implemented into the atmospheric correction program within the processing software for the fourth reprocessing of the SeaWiFS data set (Chapt. 4).

9.2 METHODS

The development of an algorithm that couples to the Gordon and Wang (1994) atmospheric correction involves several components. The first involves identifying the necessary change in the atmospheric correction. The second

involves the theory and bio-optical models used to determine the water-leaving radiance $L_W(\lambda_r)$, and third is the iterative process.

9.2.1 NIR Concept

Gordon and Wang (1994) (henceforth referred to as GW94) describe the solution for $L_t(\lambda)$:

$$L_t(\lambda) \;=\; L_r(\lambda) \;+\; [L_a(\lambda) \;+\; L_{\rm ra}(\lambda)] \;+\; t(\lambda)L_W(\lambda), \quad (35)$$

where $L_t(\lambda)$ is the radiance at the top of the atmosphere, $L_r(\lambda)$ is the Rayleigh scattering radiance, $L_a(\lambda)$ is the aerosol scattering radiance, $L_{\rm ra}(\lambda)$ is the interaction between molecular and aerosol scattering radiance, $t(\lambda)$ is the diffuse transmittance through the atmosphere, and $L_W(\lambda)$ is the water-leaving radiance. A basic assumption of the GW94 atmospheric correction approach is that $L_W(\lambda_r)$ is negligible. This assumption allows for the selection of an aerosol model using

$$L_a(\lambda_r) \;+\; L_{\rm ra}(\lambda_r) \;=\; L_t(\lambda_r) \;-\; L_r(\lambda_r). \quad (36)$$

If $L_W(765)$ and $L_W(865)$ are not negligible, the right side of (36) is increased, introducing two different errors in the determined aerosols. First, if $L_W(865)$ is not negligible, then $L_a(865) + L_{\rm ra}(865)$ is overestimated. This means that more aerosol is determined than is present, resulting in overcorrection for aerosols at all bands, producing $L_W(\lambda_r)$ to be lower than is the case. Second, with $L_W(765)$ not negligible, the aerosol type will be in error. The absorption by water at the SeaWiFS bands varies (Table 9), and at 765 nm it is 57% of that at 865 nm. As a result, $L_W(765) > L_W(865)$, and water-leaving radiance that is interpreted as aerosol will have a high ϵ value. For the extreme case of an atmosphere with no aerosol, water-leaving radiance at 765 and 865 nm would result in $\epsilon(765, 865) \approx 2.2$, almost double the highest value for a true aerosol reported in GW94, and much higher than $\epsilon(765, 865) \approx 1$ observed for marine aerosols. The resultant atmospheric model will lead to an overcorrection error where the overcorrection increases with shorter wavelength. Where the water already has low reflectance in the blue bands, such as in Case-2 water, the overcorrection would produce negative L_W in blue bands. Accordingly, a solution for $t(\lambda)L_W(\lambda_r)$ is needed.

9.2.2 Bio-Optical Models for NIR Iteration

Because of the strong absorption at the wavelengths of interest the relationship of remote sensing reflectance ($R_{\rm rs}$) to the inherent optical properties, backscatter (b_b) and total absorption ($a_{\rm tot}$) is reduced from the general form (adapted from (4) in Gordon et al. 1988):

$$R_{\rm rs}(\lambda) \;=\; y\frac{T_w}{Q(\lambda)}\;\frac{b_b(\lambda)}{b_b(\lambda) + a_{\rm tot}(\lambda)}, \quad (37)$$

to the linear form

$$R_{\rm rs}(\lambda) \;\simeq\; y\frac{T_w}{Q(\lambda)}\;\frac{b_b(\lambda)}{a_{\rm tot}(\lambda)}, \quad (38)$$

where in (37) and (38), T_w is the transmission and refraction loss at the air–water interface; and Q is the factor E_u/L_u, where E_u and L_u are the upwelling irradiance and radiance, respectively. The Q-factor is often assumed to be π, although the value is somewhat larger and variable. The variable y is the l_1 value from Gordon et al. (1988) times Q.

The linear form of (38) assures a stable iteration at high reflectance, although (37) shows that $R_{\rm rs}(\lambda)$ should approach $(y[T_w/Q(\lambda)])$ asymptotically without exceeding it. Ruddick et al. (2000) also showed that the linear solution is an accurate estimator of the Gordon et al. (1988) solution in the NIR.

The backscattering term (b_b), is the sum of b_b from pure water ($b_{\rm bw}$) and b_b from particles ($b_{\rm bp}$). The particle concentration and the scattering efficiency (size characteristics and the index of refraction) influence spectral b_b. Gould et al. (1999) determined that the spectral shape of b_b is linear in coastal waters. The backscatter is sufficient to produce measurable reflectance in the NIR part of the spectrum (Ruddick et al. 2000 and Siegel et al. 2000).

For the iterative solutions, $R_{\rm rs}$ is estimated at the critical NIR wavelengths, λ_r, from $R_{\rm rs}$ from a reference band, λ_j, using a solution of (38):

$$R_{\rm rs}(\lambda_r) \;=\; R_{\rm rs}(\lambda_0)\,\frac{a_{\rm tot}(\lambda_0)}{a_{\rm tot}(\lambda_r)}\,r_{\rm bb}(\lambda_r, \lambda_j), \quad (39)$$

where the backscatter relationship ($r_{\rm bb}$) is

$$r_{\rm bb}(\lambda_r, \lambda_j) \;=\; \left[\frac{b_b(\lambda_r)}{b_b(\lambda_j}\right]^{\eta}, \quad (40)$$

and η is a constant. As $b_{\rm bp} >> b_{\rm bw}$, it is only necessary to determine $r_{\rm bb}$ rather than the actual backscatter. For the two NIR bands, λ_r becomes λ_i, and λ_j is 670 nm.

Gould et al. (1999) concluded that the Petzold volume scattering function, b, varied linearly with wavelength, and $b_b \approx 0.02b$. Their result gives a spectral relationship for backscatter in coastal waters:

$$b_b(\lambda) \;=\; -0.00113\lambda \;+\; 1.62517, \quad (41)$$

with $\eta = 1$ in (40). If no spectral dependence existed, then either $\eta = 0$ or $B_0 = 0$.

The total absorption is

$$a_{\rm tot}(\lambda) \;=\; a_w(\lambda) \;+\; a_{\rm ph}(\lambda) \;+\; a_{\rm dg}(\lambda), \quad (42)$$

where a_w, $a_{\rm ph}$, and $a_{\rm dg}$ are the coefficients of absorption due to water, phytoplankton, and dissolved or detritus matter, respectively. For the 670 nm band, all three terms

are determined; for the 765 and 865 nm bands, $a_{\rm ph}$ and $a_{\rm dg}$ are presumed to be negligible.

The a_w term is determined from tabulated values from Palmer and Williams (1974) and Pope and Fry (1997), with additional data from Curcio and Petty (1951) and Smith and Baker (1981). The $a_{\rm ph}$ term is found using data from Morel and Gentili (1991) with tuning of $a_{\rm ph}(440)$ to the SeaBAM data set (O'Reilly et al. 1998, and Maritorena and O'Reilly 2000):

$$a_{\rm ph}(440) \;=\; 0.08(C_a)^{0.65}. \qquad (43)$$

Using Bricaud et al. (1998), and Lee et al. (1998) $a_{\rm ph}$ is obtained:

$$a_{\rm ph}(\lambda) \;=\; a_{\rm ph}(440)\,[A_0(\lambda) + A_1(\lambda)\,\ln a_{\rm ph}(440)]. \qquad (44)$$

While $a_{\rm ph}$ is determined everywhere; for $C_a < 1 \mu{\rm g\,L^{-1}}$, it becomes negligible as $a_{\rm ph}/a_w < 0.05$.

In coastal waters such as river plumes, detrital and gelbstoff absorption can be significant. Absorption at 400 nm of 1–20 $\rm m^{-1}$, corresponds to an absorption at 670 nm of 0.04–0.7 $\rm m^{-1}$, which is greater than $a_{\rm dg}(400)$ in some Case-1 waters. An analysis of field data has shown that the $a_{\rm dg}$ value may be approximated by using the 555 and 670 nm bands. For coastal waters, which includes waters having extremely high $a_{\rm dg}$ values, the extreme absorption in the blue eliminates the information content of the 412 and 443 nm bands for determining $a_{\rm dg}(412)$ (Carder et al. 1999). As a result, a semi-analytical solution is employed using the 555 and 670 nm bands, using the ratio of $R_{\rm rs}(555)$ and $R_{\rm rs}(670)$, where

$$a_{\rm dg}(670) \;=\; 0.147 \;-\; 0.18X, \qquad (45)$$

when

$$X \;=\; \frac{R_{\rm rs}(555) \;-\; R_{\rm rs}(670)}{R_{\rm rs}(555)}. \qquad (46)$$

The coefficients in (44) were determined by fitting X to derived $a_{\rm dg}$ (Fig. 33). The effectiveness of this method is shown from field data where it is dominated by $a_{\rm dg}$ (Fig. 34). For areas offshore, $a_{\rm dg}(670)$ is negligible. An additional analysis compared estimated $R_{\rm rs}(412)$ [using (41)–(46) in (38)] to observed $R_{\rm rs}(412)$, including water with extremely high dissolved absorption. The solution uses $a_{\rm dg}(412) = a_{\rm dg}(670)\exp[0.013(670-412)]$. The comparison shows the ability to estimate $a_{\rm dg}(670)$ is meaningful even when using it to extrapolate to 412 nm (Fig. 35).

9.2.2.1 NIR Iteration Application

In the SeaWiFS processing, (39) was implemented using an iterative computation of $L_W(765)$ and $L_W(865)$. The procedure is based on the original SeaWiFS processing code using the GW94 atmospheric model. The goal is to remove the $L_W(\lambda_r)$ component from $L_t(\lambda_r)$, so that only the atmospheric component of $L_t(\lambda_r)$ is input into GW94. The iteration first uses $L_t(\lambda_r)$ as input to GW94 in order to solve for $L_W(670)$, as would be done in any noniterative method. Then, $L_W(670)$ is used through the model described in (39) to determine $L_W(\lambda_r)$ [i.e., $L_W(765)$ and $L_W(865)$]. These are propagated to the top of the atmosphere (correcting L_W for the direct transmittance $T(\lambda)$ determined from the GW94 atmospheric model). This TOA $L_W(\lambda_r)$ is removed from $L_t(\lambda_r)$ which is then input into the GW94 computation.

0-iteration:
$L_t(\lambda_r)$ is input into GW94, whose output goes into $R_{\rm rs}(\lambda_v)$, where (λ_v) are the visible wavelengths; $R_{\rm rs}(670)$ is input into (39), whose output $R_{\rm rs}(\lambda_r)$ is

$$L_t(\lambda_r)_1 \;=\; L_t(\lambda_r) \;-\; T(\lambda_r)\,R_{\rm rs}(\lambda_r)_0\,F_0(\lambda_r). \qquad (47)$$

1-iteration:
$L_t(\lambda_r)_1$ is input into GW94, the output of which goes into $R_{\rm rs}(\lambda_v)_1$; $R_{\rm rs}(670)_1$ is input into (39), whose output $R_{\rm rs}(\lambda_r)_1$ is

$$L_t(\lambda_r)_2 \;=\; L_t(\lambda_r)_1 \;-\; T(\lambda_r)\,R_{\rm rs}(\lambda_r)_1\,F_0(\lambda_r). \qquad (48)$$

If $\Delta R_{\rm rs}(765) = R_{\rm rs}(\lambda_{\rm ir})_1 - R_{\rm rs}(\lambda_{\rm ir})_0 > 10^{-5}\,{\rm sr^{-1}}$ then continue the iteration; else stop the iteration.

The iteration is not performed if the initial $R_{\rm rs}(765) < 5\times10^{-5}{\rm sr^{-1}}$ or if $L_W(670) < 0$, and the iteration stops when $\Delta R_{\rm rs}(765)$ (the change between iterations) is less than $10^{-5}\,{\rm sr^{-1}}$.

The minimum threshold to initiate iteration constrains the solution to water having a significant scattering signal. Even in oligotrophic Case-1 water, such as the Loop Current in the Gulf of Mexico, SeaWiFS has sufficient sensitivity that two iterations could be performed if some constraint were not applied. The process is run for up to eight iterations; although convergence is generally achieved in two iterations, and rarely takes more than four.

The atmospheric error tends to cause a greater error at shorter wavelengths, which has a potential impact on the iterative solution. The underestimate results in the C_a and $a_{\rm ph}$ being overestimated. To prevent overestimation of $a_{\rm tot}(670)$ and the resultant overcorrection, the C_a concentrations in the computation are limited on the first two iterations. The C_a value is not allowed to be greater than $10\,\mu{\rm g\,L^{-1}}$ as an input to the computation of the first iteration, and not greater than $20\,\mu{\rm g\,L^{-1}}$ in the computation of the second iteration. (The C_a product is not limited in any way.) If $L_W(555) < 0$ during any iteration, then only $a_w(670)$ is used in the computation of $a_{\rm tot}(670)$, as neither $a_{\rm ph}(670)$ nor $a_{\rm dg}(670)$ is determined. In most areas, C_a and detrital–gelbstoff absorption are not as critical as water absorption in determining $a_{\rm tot}(670)$. In some estuaries and river plumes, detrital and dissolved absorption produce a significant effect.

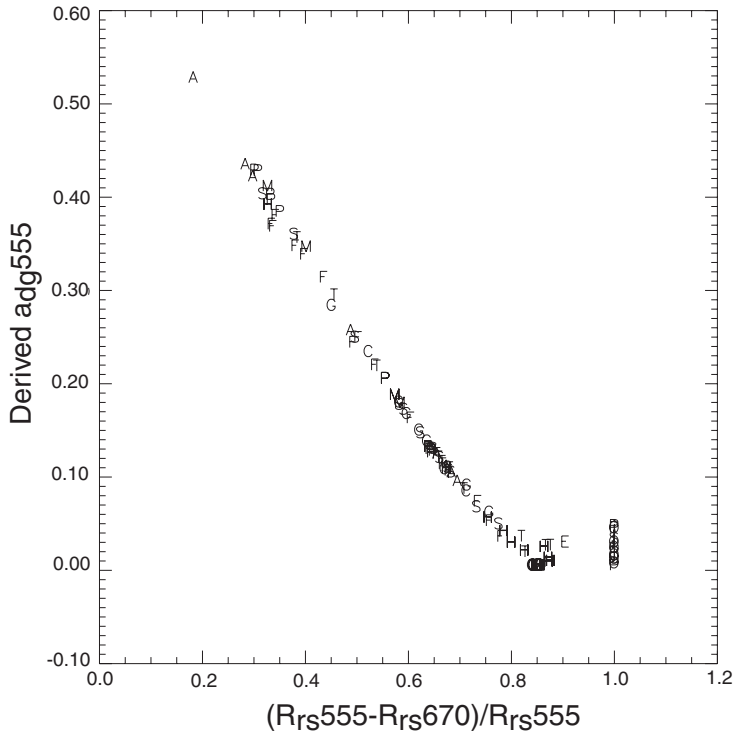

Fig. 33. Comparison of $X = [R_{\rm rs}(555) - R_{\rm rs}(670)]/R_{\rm rs}(555)$ to $a_{\rm dg}(555)$ derived from spectral model. The labels indicate locations of field data: `P`=Pamlico, `T`=Tampa Bay, `A`=Alabama shelf, `F`=Florida Bay, `S`=South Atlantic Bight, `G`= Gulf of Mexico, `H`=North Carolina shelf; the best fit to this solution is (45). The derived $a_{\rm dg}$ came from the total absorption, (38), less the phytoplankton absorption, (44).

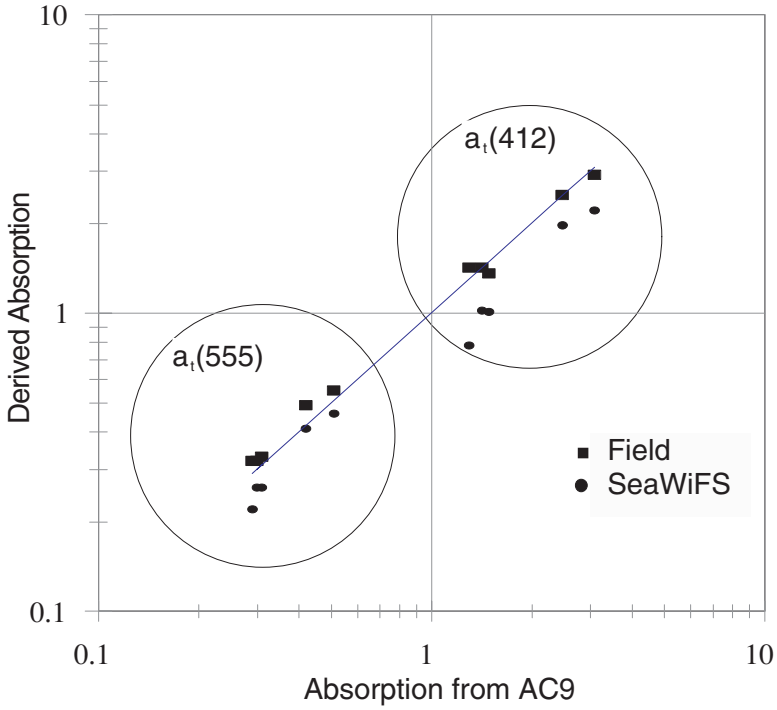

Fig. 34. The derived total absorption ($a_{\rm tot}$) at 412 and 555 nm compared with AC-9. The coastal $a_{\rm dg}$ computation applies at these sites and $a_{\rm dg}$ produces over 90% of the total absorption at these bands. The derived total absorption ($a_{\rm tot}$) used $R_{\rm rs}$ with (44) and (45).

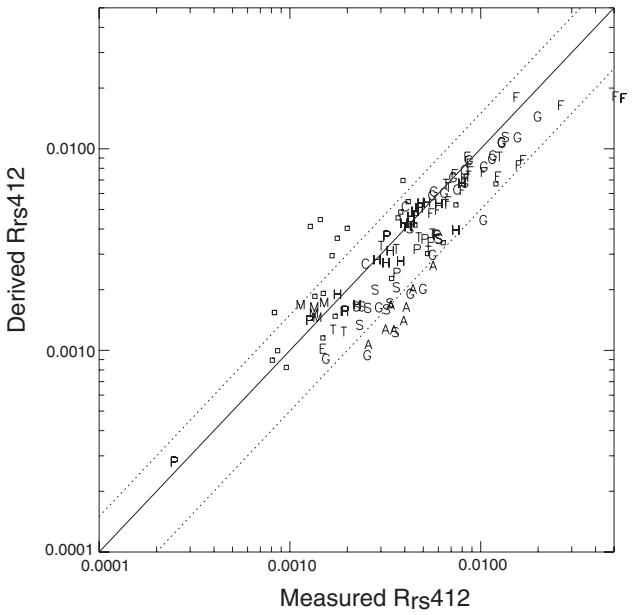

Fig. 35. Estimated $R_{\rm rs}(412)$ versus observed $R_{\rm rs}(412)$ using the Gulf of Mexico–South Atlantic Bight data set developed as part of this study. The SeaBAM tuning was applied here. The boxes are samples that did not have a 670 nm value, so the coastal $a_{\rm dg}$ could not be used. The letters denoting locations are the same as in Fig. 33. The estimate accounts for 83% of the variance in the measured $R_{\rm rs}(412)$.

The iterative solutions were implemented in the SeaWiFS Data Analysis System (SeaDAS) version 4 and were applied to pixels containing the station taken within one day of the sample. The standard calibration was applied. The C_a value was found using version 2 of the Ocean Chlorophyll (OC2) algorithm (Maritorena and O'Reilly 2000).

9.3 RESULTS

SeaWiFS imagery was processed using the iterative technique for the northern Gulf of Mexico, South Atlantic Bight, and the East Coast. In the coastal zone of the Gulf of Mexico, scattering due to suspended particulate matter is significant, as well as absorption from dissolved and detrital materials.

The NIR iteration produces a substantial decrease in the correlation of $L_a(865)$ with $L_W(670)$ (Figs. 36 and 37). Without the NIR iteration, a strong correlation exists between aerosol radiance and water-leaving radiance [the smallest values of $L_a(865)$ for each $L_a(670)$]. For pixels with the lowest aerosol, $L_a(865)$ increased at about $0.07L_W(670)$ with a noniterative process. After the iteration, most of the correlation has been removed, with $L_a(865)$ showing a negligible change for $L_W(670) < 1.5\,\mathrm{mW\ cm^{-2}\,\mu m^{-1}\,sr^{-1}}$ (or $R_{\rm rs}(670) < 0.0096\,\mathrm{sr^{-1}}$). The $L_a(865)$ value shows a weak correlation for greater $L_W(670)$, with $L_a(865)$ changing at approximately $0.015\times$ Ł$_W(670)$. These areas are among the highest scattering found, including the core Mississippi River plume and Florida Bay during major resuspension events (of calcium carbonate sediments). The linearization of the relationship of $R_{\rm rs}$ to the optical properties (b_b and a) in (39) produces a negligible effect for low $R_{\rm rs}(670)$. Ruddick et al. (2000) noted that for the ratio of NIR reflectances, the linearized form produced only small errors.

A comparison of the iterative and noniterative method shows that the iterative techniques increase reflectance at shorter wavelengths (Fig. 38). The noniterative and Siegel process produces a strong spectrally dependent bias against field measurements (Fig. 39), while the NIR iteration reduces both the bias and the RMS error against the measured data (Figs. 39 and 40). With the reduction in the spectral component of the bias, the calculated C_a value from SeaWiFS becomes more consistent with that calculated from field radiometry (Fig. 41).

In order to prevent iteration from occurring unnecessarily in extremely clear waters, iteration does not take place if $R_{\rm rs}(765) > 5\times10^{-5}$. This suggests that some NIR water-leaving radiance may be present in most Case-1 water (Siegel et al. 2000). The iteration is based on the spectral characteristic of backscatter by inorganic sediments. In Case-1 water (which does not have inorganic scattering), the spectral backscatter relationship, $r_{\rm bb}(\lambda_r, 670)$, will be influenced by phytoplankton and may differ from that used here. Phytoplankton tends to produce much less backscatter than inorganic particles, so the errors in using a sediment-based $r_{\rm bb}(\lambda_r, 670)$ may be small, even though phytoplankton does produce some NIR scattering (Siegel et al. 2000). The potential for error, however, in high chlorophyll Case-1 waters should be examined.

The NIR iteration does not remove all negative radiances, indicating that other factors, probably absorbing aerosols, are also involved in this error (Figs. 39 and

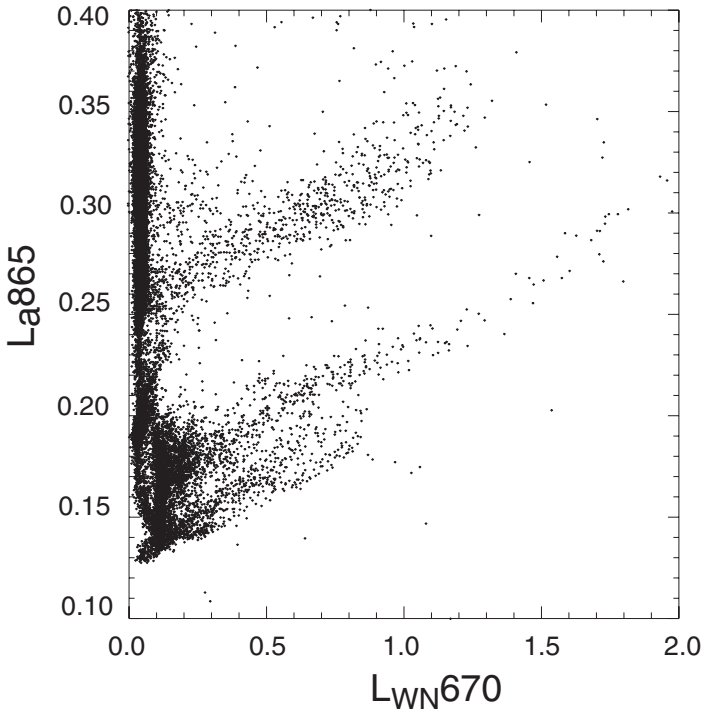

Fig. 36. Comparison of $L_a(865)$ with a $L_{WN}(670)$ with a standard noniterative process indicating correlation of presumed aerosol with water-leaving radiance (in units of $\mathrm{mW\,cm^{-2}\,\mu m^{-1}\,sr^{-1}}$).

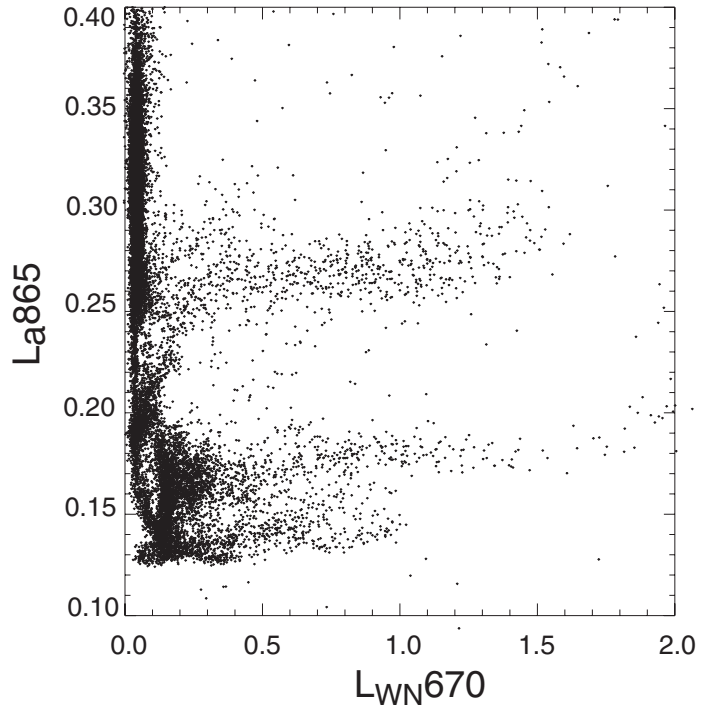

Fig. 37. Comparison of $L_a(865)$ with the NIR iteration, compare with Fig. 38 to show the decrease in correlation between the presumed aerosol and water-leaving radiance (in units of $\mathrm{mW\,cm^{-2}\,\mu m^{-1}\,sr^{-1}}$).

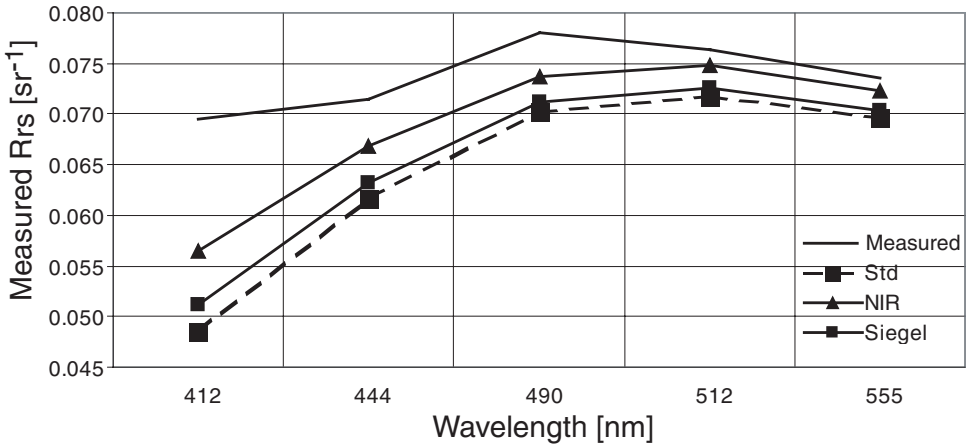

Fig. 38. Mean spectra of noniterative (standard), Siegel iteration, and NIR-iteration methods of processing SeaWiFS data are shown in the station data from the Gulf of Mexico and South Atlantic Bight. The 64 stations were taken over a two-year period.

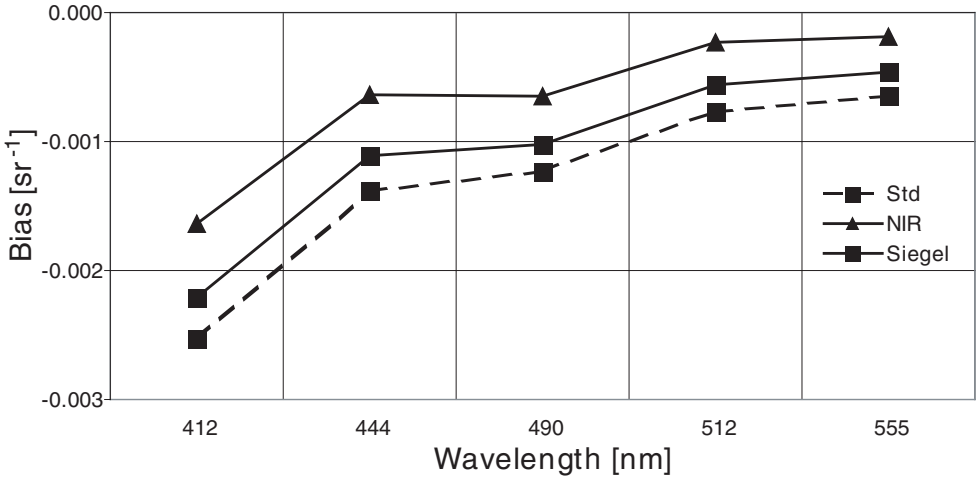

Fig. 39. Bias of SeaWiFS-derived reflectances against measured reflectances taken within one day of overpasses for the noniterative (standard), Siegel iteration, and NIR-iteration methods.

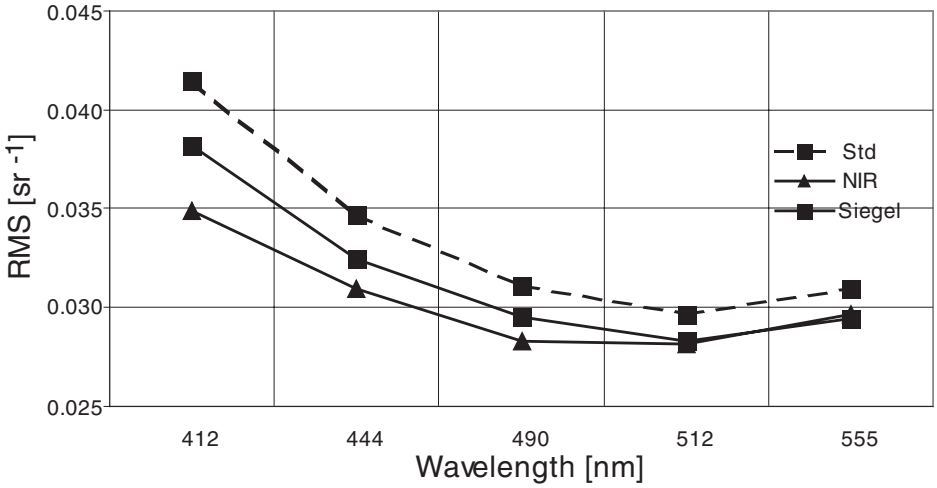

Fig. 40. RMS error between SeaWiFS and field reflectances taken within one day of overpasses for the noniterative (standard), Siegel iteration, and NIR-iteration methods.

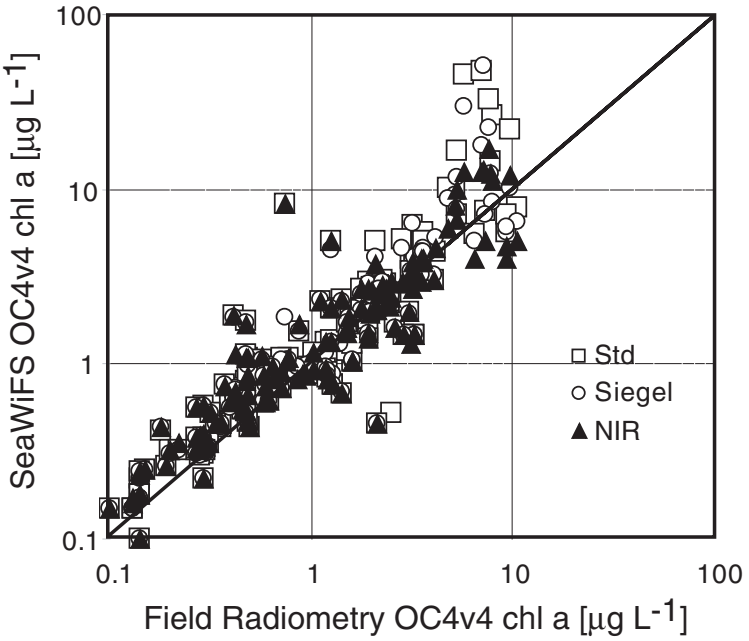

Fig. 41. Comparison of chlorophyll estimated by the Ocean Chlorophyll 4 version 4 algorithm (OC4v4) from satellite- and field matchups for the noniterative (standard), Siegel iteration, and NIR-iteration methods.

40). By improving the aerosol model selection, however, the algorithm results in less error, particularly at shorter wavelengths. As expected, once the scattering effect was removed, the calculated C_a from the OC2 algorithm decreased. The NIR iteration produces a substantial decrease in C_a value in coastal waters. The C_a algorithm is based on the ratio, $R_{\rm rs}(490)/R_{\rm rs}(555)$, and the errors reduce $R_{\rm rs}(490)$ relative to $R_{\rm rs}(555)$. Removing the scattering effect removes this error, bringing the C_a value to reasonable levels.

9.4 CONCLUSIONS

This chapter has described an atmospheric correction procedure that will extend SeaWiFS products into the coastal regions. This procedure provides an improved method of estimating the water-leaving radiance and remote sensing reflectance in turbid coastal waters. This procedure is partially coupled with the Gordon and Wang solution for scattering and molecular absorption and is based on semi-analytic solutions to the spectral behavior of the remote sensing reflectance of the water. This interation presumed a fixed spectral shape of the backscatter, $r_{\rm bb}(\lambda_r, 670)$. In water that is dominated by chlorophyll, this shape may change somewhat.

The full correction described here improves the accuracy of retrieval of remote sensing reflectance, which inherently reduces the number of pixels with unacceptably low reflectances. It will further permit extension of image products into bays and estuaries, however, it will not eliminate all negative radiance. Areas of highly turbid coastal water that produce negative radiances at 555 nm will require additional algorithms to achieve a valid atmospheric correction.

Glossary

ACS Attitude Control System
AOT Aerosol Optical Thickness

BBOP Bermuda BioOptics Project

CVT Calibration and Validation Team
CZCS Coastal Zone Color Scanner

DAAC Distributed Active Archive Center

ETOPO2 Earth Topography 2 min grid
ETOPO5 Earth Topography 5 min grid

GAC Global Area Coverage (SeaWiFS 1 km resolution, subsampled to 4 km)
GPS Global Positioning System
GSFC Goddard Space Flight Center

HRPT High Resolution Picture Transmission

LAC Local Area Coverage (SeaWiFS 1 km resolution)

MERIS Medium Resolution Imaging Spectrometer
MOBY Marine Optical Buoy
MODIS Moderate Resolution Imaging Spectroradiometer

NASA National Aeronautics and Space Administration
NDVI Normalized Difference Vegetation Index
NEC Northeast US Coastal Ecosystem
NIR Near-Infrared
NIST National Institute of Standards and Technology

OCTS Ocean Color and Temperature Scanner
OrbView-2 Not an acronym, but the current name for the SeaStar satellite.

PAR Photosynthetically Available Radiation

QC Quality Control

RMA Reduced Major Axis
RMS Root Mean Squared
ROLO Robotic Lunar Observatory
RSR Relative Spectral Response

SBRS Santa Barbara Research Systems
SeaDAS SeaWiFS Data Analysis System
SeaWiFS Sea-viewing Wide Field-of-view Sensor
SIMBIOS Sensor Intercomparison and Merger for Biological and Interdisciplinary Oceanic Studies
SIRCUS Spectral Irradiance and Radiance Responsitivity Calibrations Using Uniform Standards

TOA Top of the Atmosphere

USGS United States Geological Survey
UTC Coordinated Universal Time

Symbols

a_0 Coefficient of the lunar calibration function of time.
a_1 Coefficient of the lunar calibration function of time.
a_2 Coefficient of the lunar calibration function of time.
a_{dg} Absorption coefficient for detritus and gelbstoff.
a_{oz} Ozone absorption coefficient.
a_p Absorption coefficient for particles.
a_{ph} Absorption coefficient for phytoplankton.
a_{tot} Total absorption coefficient, the sum of a_{dg}, a_p, and a_w.
a_w Absorption coefficient for water.
A Cloud–surface system albedo.
A_s Albedo of the ocean surface.

b Scattering function.
b_b Backscatter coefficient.
b_{bp} Particulate backscatter coefficient.
b_{wv} Pure water backscatter coefficient.

C_a Chlorophyll a concentration.
C_{oz} Ozone concentration.

d_a Distance of aerosol model.

E_0 Solar flux at the top of the atmosphere.
E_c Solar flux that would reach the surface if the cloud–surface system were nonreflecting and nonabsorbing.
E_s Solar flux reaching the ocean surface.
$\bar{E}_s$ Estimate of daily PAR.
E_u Upwelling radiance.
$\bar{E}_\theta$ Mean extraterrestrial solar irradiance.

f Lunar calibration function of time.
f_T Detector temperature correction.
f/Q Bidirectional reflectance at the water's surface.
F Dependence of the cloud–surface system albedo on solar zenith angle.
F_0 Solar irradiance.

G_i Gain for a given band.

i An index variable for either a given pixel, band, or number of iterations.
i_c Centered pixel i.

j An index variable for a given band.

k SeaWiFS aerosol model indicator.
K_2 Detector temperature correction factor.
$K_d(490)$ Diffuse attenuation coefficient at 490 nm.

l_1 SeaWiFS aerosol model indicator.
$L(\lambda_M)$ The L_{WN} values for MOBY.
$L(\lambda_S)$ The L_{WN} values for SeaWiFS.
$L(\lambda_{S/M})$ $L(\lambda_S)$ averaged over the 5×5 pixel subscene and this average value is divided by $L(\lambda_M)$.
$L_a(\lambda, i)$ Aerosol path radiance, including Rayleigh-aerosol interaction for wavelength λ at location i.
$L'_a(\lambda, i)$ The computed aerosol path radiance, including Rayleigh-aerosol interaction for wavelength λ at location i.
$L_r(\lambda, i)$ Rayleigh path radiance for wavelength λ at location i.
L_{ra} Interaction between molecular and aerosal scattering radiance.
L_t Radiance at the top of the atmosphere.
$L_t(\lambda, i)$ Observed TOA radiance for wavelength λ at location i.
L_u Upwelling radiance.
L_W Water-leaving radiance.
$L_{WN}(\lambda)$ Normalized water-leaving radiance at wavelength λ.
$L_{WN}(\lambda_r)$ Normalized water-leaving radiance in the NIR part of the spectrum.
L'_{WN} Corrected normalized water-leaving radiance.
$L_{WN}(0^-)$ Normalized water-leaving radiance, just below the sea surface.
$L_{WN}(0^+)$ Normalized water-leaving radiance, just above the sea surface.

n_w Refractive index of the water.
N Number of matchups.

P_a Aerosol phase function.
P_m Molecular phase function.
$P_{\rm neg}(\lambda)$ Percent frequency of pixels with negative water-leaving radiances.

Q The factor E_u/L_u.

$r_{\rm bb}$ Backscatter relationship.
R^2 Coefficient of determination.
$R_{\rm rs}(\lambda)$ Remote-sensing reflectance at wavelength λ.

S_a Spherical albedo.

t Time.
$t(\lambda)$ Diffuse transmittance.
t_d Clear sky total (diffuse + direct) transmittance.
$t_f(\theta)$ Fresnel transmittance of the air–sea interface.
t_g Gaseous transmittance.
$tL_f(\lambda, i)$ White-cap radiance, transmitted to the TOA for wavelength λ at location i.
$t_{\rm ox}(\lambda, i)$ Oxygen transmittance for wavelength λ at location i.
$t_{\rm oz}$ Gaseous transmittance due to ozone.
$t_{\rm oz}(\lambda, i)$ Ozone transmittance for wavelength λ at location i.
$t_{\rm wv}$ Gaseous transmittance due to water vapor.
t_0 Reference time for lunar calibration time series.
T Detector temperature.
$T(\lambda)$ Direct transmittance.
T_d Clear sky direct transmittance.
$T_{\rm ref}$ Detector reference temperature.
T_w Transmission and refraction loss at the air–water interface.

X See (46).

y The l_1 value from Gordon et al. (1988) times Q.

α Ångström coefficient.

ϵ Single-scattering aerosol reflectance ratio.
$\epsilon_{\rm ms}$ Multiscattering equivalent of ϵ.

η Constant.

θ Sensor zenith angle.
θ_0 Solar zenith angle.
θ_v Viewing zenith angle.

λ Wavelength.
λ_i Nominal wavelength for band i.
$\lambda_{i/j}$ Radiance ratio of band i to band j.
λ_j Reference band wavelength.
λ_M The L_{WN} values for MOBY.
λ_r The NIR part of the spectrum.
λ_S The L_{WN} values for SeaWiFS.
$\lambda_{S/M}$ Mean of the SeaWiFS and MOBY L_{WN} values.
λ_v Wavelength in the visible part of the spectrum.

ρ_a Aerosol path reflectance at wavelength λ.
$\rho_{\rm atm}$ Reflectance due to scattering by molecules and aerosols in the atmosphere.
ρ_s Reflectance of the cloud–surface layer.
ρ_t Reflectance at the top of the atmosphere.
ρ'_t Corrected ρ_t for gaseous absorption due to ozone.

τ_a Aerosol optical thickness.
τ_m Optical thickness of molecules.

ω_a Single scattering albedo of aerosols.

References

Ainsworth, E.J., and F.S. Patt, 2000: "Modifications to the TOMS ozone ancillary data interpolation." In: McClain, C.R., E.J. Ainsworth, R.A. Barnes, R.E. Eplee, Jr., F.S. Patt, W.D. Robinson, M. Wang, and S.W. Bailey, SeaWiFS Postlaunch Calibration and Validation Analyses, Part 1. *NASA Tech. Memo. 2000–206892, Vol. 9,* S.B. Hooker and E.R. Firestone, Eds., NASA Goddard Space Flight Center, Greenbelt, Maryland, 69–73.

Bailey, S.W., C.R. McClain, P.J. Werdell, and B.D. Schieber, 2000: "Normalized water-leaving radiance and chlorophyll *a* match-up analyses." In: McClain, C.R., R.A. Barnes, R.E. Eplee, Jr., B.A. Franz, N.C. Hsu, F.S. Patt, C.M. Pietras, W.D. Robinson, B.D. Schieber, G.M. Schmidt, M. Wang, S.W. Bailey, and P.J. Werdell, SeaWiFS Postlaunch Calibration and Validation Analyses, Part 2. *NASA Tech. Memo. 2000–206892, Vol. 10,* S.B. Hooker and E.R. Firestone, Eds., NASA Goddard Space Flight Center, Greenbelt, Maryland, 45–52.

Barnes, R.A., A.W. Holmes, W.L. Barnes, W.E. Esaias, C.R. McClain, and T. Svitek, 1994: SeaWiFS Prelaunch Radiometric Calibration and Spectral Characterization. *NASA Tech. Memo. 104566, Vol. 23,* S.B. Hooker, E.R. Firestone, and J.G. Acker, Eds., NASA Goddard Space Flight Center, Greenbelt, Maryland, 55 pp.

——, ——, and W.E. Esaias, 1995: Stray Light in the SeaWiFS Radiometer. *NASA Tech. Memo. 104566, Vol. 31,* S.B. Hooker, E.R. Firestone, and J.G. Acker, Eds., NASA Goddard Space Flight Center, Greenbelt, Maryland, 76 pp.

——, R.E. Eplee, Jr., G.M. Schmidt, F.S. Patt, and C.R. McClain, 2001: Calibration of SeaWiFS. I. Direct techniques. *Appl. Opt.,* **40,** 6,682–6,700.

Bricaud, A., A. Morel, M. Babin, K. Allali, and H. Claustre, 1998: Variations of light absorption by suspended particles with chlorophyll *a* concentration in oceanic (Case-1) waters: Analysis and implications for bio-optical models. *J. Geophys. Res.,* **103,** 31,033–31,044.

Briegleb, B.P., and V. Ramanathan, 1982: Spectral and diurnal variations in clear sky planetary albedo. *J. Climate Appl. Meteor.,* **21,** 1,168–1,171.

Carder, K.L., F.R. Chen, Z.P. Lee, and S.K. Hawes, 1999: Semi-analytic Moderate-Resolution Imaging Spectrometer algorithms for chlorophyll *a* and absorption with bio-optical domains based on nitrate-depletion temperatures. *J. Geophys. Res.,* **104,** 5,403–5,421.

Clark, D.K., M.E. Feinholz, M.A. Yarbrough, B.C. Johnson, S.W. Brown, Y.S. Kim, and R.A. Barnes, 2001: "Overview of the radiometric calibration of MOBY." In: Earth Observing Systems VI, *SPIE,* **4483,** 64–76.

Curcio, J.A., and C.C. Petty, 1951: The near infrared absorption spectrum of liquid water. *J. Opt. Soc. Amer.,* **41,** 302–305.

Dedieu, G., P.-Y. Deschamps, and Y.H. Kerr, 1987: Satellite estimation of solar irradiance at the surface of the earth and of surface albedo using a physical model applied to Meteosat data. *J. Climate Appl. Meteor.,* **26,** 79–87.

Eplee, R.E., Jr., and R.A. Barnes, 2000: "Lunar data analysis for SeaWiFS calibration." In: McClain, C.R., E.J. Ainsworth, R.A. Barnes, R.E. Eplee, Jr., F.S. Patt, W.D. Robinson, M. Wang, and S.W. Bailey, SeaWiFS Postlaunch Calibration and Validation Analyses, Part 1. *NASA Tech. Memo. 2000–206892, Vol. 9,* S.B. Hooker and E.R. Firestone, Eds., NASA Goddard Space Flight Center, Greenbelt, Maryland, 17–27.

——, and C.R. McClain, 2000: "MOBY data analysis for the vicarious calibration of SeaWiFS bands 1–6." In: McClain, C.R., E.J. Ainsworth, R.A. Barnes, R.E. Eplee, Jr., F.S. Patt, W.D. Robinson, M. Wang, and S.W. Bailey, 2000: SeaWiFS Postlaunch Calibration and Validation Analyses, Part 1. *NASA Tech. Memo. 2000–206892, Vol. 9,* S.B. Hooker and E.R. Firestone, Eds., NASA Goddard Space Flight Center, Greenbelt, Maryland, 43–50.

——, W.D. Robinson, S.W. Bailey, D.K. Clark, P.J. Werdell, M. Wang, R.A. Barnes, and C.R. McClain, 2001: Calibration of SeaWiFS. II. Vicarious techniques. *Appl. Opt.,* **40,** 6,701–6,718.

Frouin, R., D.W. Lingner, K. Baker, C. Gautier, and R. Smith, 1989: A simple analytical formula to compute clear sky total and photosynthetically available solar irradiance at the ocean surface. *J. Geophys. Res.,* **94,** 9,731–9,742.

——, and B. Chertock, 1992: A technique for global monitoring of net solar irradiance at the ocean surface. Part I: Model. *J. Appl. Meteor.,* **31,** 1,056–1,066.

Fu, G., K.S. Baith, and C.R. McClain, 1998: SeaDAS: The SeaWiFS Data Analysis System. *Proc. 4th Pacific Ocean Remote Sensing Conf.,* Qingdao, China, 28–31 July 1998, 73–79.

Gordon, H.R., 1995: Remote sensing of ocean color: a methodology for dealing with broad spectral bands and significant out-of-band response. *Appl. Opt.,* **34,** 8,363–8,374.

——, and D.K. Clark, 1981: Clear water radiances for atmospheric correction of coastal zone color scanner imagery. *Appl. Opt.,* **20,** 4,175–4,180.

——, ——, J.W. Brown, O.B. Brown, R.H. Evans, and W.W. Broenkow, 1983: Phytoplankton pigment concentrations in the Middle Atlantic bight: comparison between ship determinations and Coastal Zone Color Scanner estimates. *Appl. Opt.,* **22,** 20–26.

——, O.B. Brown, R.H. Evans, J.W. Brown, R.C. Smith, K.S. Baker, and D.K. Clark, 1988: A semianalytic radiance model of ocean color. *J. Geophys. Res.,* **93,** 10,909–10,924.

——, and M. Wang, 1994: Retrieval of water-leaving radiance and aerosol optical thickness over the oceans with SeaWiFS: a preliminary algorithm. *Appl. Opt.,* **33,** 443–452.

Gould, R.W., and R.A. Arnone, 1994: Extending Coastal Zone Color Scanner estimates of the diffuse attenuation coefficient into case II waters. *SPIE, Ocean Optics XII,* **2258,** 342–356.

——, ——, and M. Sydor, 1998: Testing a new remote sensing reflectance algorithm to estimate absorption and scattering in Case-2 Waters. [Available on CD-ROM], *SPIE Ocean Optics XII,* Hawaii.

——, ——, and P.M. Martinolich, 1999: Spectral dependence of the scattering coefficient in Case-1 and Case-2 waters. *Appl. Opt.,* **38,** 2,377–2,383.

Hale, G.M., and M.R. Query, 1973: Optical constants of water in the 200-nm to 200μm wavelength region. *Appl. Opt.,* **12,** 555–563.

Hu, C., K.L. Carder, and F.E. Müeller-Karger, 2000a: How precise are SeaWiFS ocean color estimates? Implications of digital noise errors. *Remote Sens. Environ.,* **76,** 239–249.

——, ——, and ——, 2000b: Atmospheric correction of SeaWiFS imagery over turbid coastal waters; a practical method. *Remote Sens. Environ.,* **74,** 195–206.

Kieffer, H.H., T.C. Stone, R.A. Barnes, S. Bender, R.E. Eplee, Jr., J. Mendenhall, and L. Ong, 2002: "On-orbit radiometric calibration over time and between spacecraft using the Moon." In: Sensors, Systems, and Next Generation Satellites VIII, *SPIE,* **4881**, 301–313.

Kirk, J.T.O., 1994: *Light and Photosynthesis in Aquatic Ecosystems,* 2nd edition, Cambridge University Press, 509 pp.

Kou, L., D. Labrie, and P. Chylek, 1993: Refractive indices of water and ice in the 0.65-2.5 μm spectral range. *Appl. Opt.,* **32,** 3,531–3,540.

Land, P.E., and J.D. Haigh, 1996: Atmospheric correction over case 2 waters with an iterative fitting algorithm, *Appl. Opt.,* **35,** 5,443–5,451.

Lee, Z.P., K.L. Carder, R.G. Steward, T.G. Peacock, C.O. Davis, and J.S. Patch, 1998: An empirical ocean color algorithm for light absorption coefficients of optically deep waters. *J. Geophys. Res.,* **103,** 27,967–27,978.

Loisel, H., and A. Morel, 1998: Light scattering and chlorophyll concentration in Case-1 water: a reexamination. *Limnol. Oceanogr.,* **43,** 847–858.

Maritorena, S., and J.E. O'Reilly, 2000: "OC2v2: Update on the initial operational SeaWiFS chlorophyll *a* algorithm." In: O'Reilly, J.E., and 24 Coauthors, SeaWiFS Postlaunch Calibration and Validation Analyses, Part 3. *NASA Tech. Memo. 2000–206892, Vol. 11,* S.B. Hooker and E.R. Firestone, Eds., NASA Goddard Space Flight Center, Greenbelt, Maryland, 3–8.

McClain, C.R., 2000: "SeaWiFS postlaunch calibration and validation overview." In: McClain, C.R., E.J. Ainsworth, R.A. Barnes, R.E. Eplee, Jr., F.S. Patt, W.D. Robinson, M. Wang, and S.W. Bailey, SeaWiFS Postlaunch Calibration and Validation Analyses, Part 1. *NASA Tech. Memo. 2000–206892, Vol. 9,* S.B. Hooker and E.R. Firestone, Eds., NASA Goddard Space Flight Center, Greenbelt, Maryland, 4–12.

——, E.J. Ainsworth, R.A. Barnes, R.E. Eplee, Jr., F.S. Patt, W.D. Robinson, M. Wang, and S.W. Bailey, 2000a: SeaWiFS Postlaunch Calibration and Validation Analyses, Part 1. *NASA Tech. Memo. 2000–206892, Vol. 9,* S.B. Hooker and E.R. Firestone, Eds., NASA Goddard Space Flight Center, Greenbelt, Maryland, 82 pp.

——, R.A. Barnes, R.E. Eplee, Jr., B.A. Franz, N.C. Hsu, F.S. Patt, C.M. Pietras, W.D. Robinson, B.D. Schieber, G.M. Schmidt, M. Wang, S.W. Bailey, and P.J. Werdell, 2000b: SeaWiFS Postlaunch Calibration and Validation Analyses, Part 2. *NASA Tech. Memo. 2000–206892, Vol. 10,* S.B. Hooker and E.R. Firestone, Eds., NASA Goddard Space Flight Center, Greenbelt, Maryland, 57 pp.

——, R. Evans, J. Brown, and M. Darzi, 1995: "SeaWiFS Quality Control Masks and Flags: Initial Algorithms and Implementation Strategy," In: McClain, C.R., W.E. Esaias, M. Darzi, F.S. Patt, R.H. Evans, J.W. Brown, K.R. Arrigo, C.W. Brown, R.A. Barnes, and L. Kumar: SeaWiFS Algorithms, Part 1. *NASA Tech. Memo. 104566, Vol. 28,* S.B. Hooker, E.R. Firestone, and J.G. Acker, Eds., NASA Goddard Space Flight Center, 3–7.

Moore, G.K., 1980: Satellite remote sensing of water turbidity. *Bull. Hydrolog. Sci.,* **25,** 407–421.

——, J. Aiken, and S.J. Lavender, 1999: The atmospheric correction of water colour and the quantitative retrieval of suspended particulate matter in Case II waters application to MERIS, *Int. J. Remote Sens.,* **20,** 1,713–1,734.

Morel, A., 1988: Optical modeling of the upper ocean in relation to its biogenous matter content (Case-1 waters). *J. Geophys. Res.,* **93,** 10,749–10,768.

——, and B. Gentili, 1991: Diffuse reflectance of oceanic waters: its dependence on sun angle as influenced by the molecular scattering contribution. *Appl. Opt.* **30,** 4,427–4,438.

——, and S. Maritorena, 2001: Bio-optical properties of oceanic waters: A reappraisal. *J. Geophys. Res.,* **106,** 7,163–7,180.

——, and J.L. Mueller, 2002: "Normalized water-leaving radiance and remote sensing reflectance: Bidirectional reflectance and other factors." In: J.L. Mueller and G.S. Fargion, Eds., Ocean Optics Protocols for Satellite Ocean Color Sensor Validation, Revision 3, Vol. 2. *NASA Tech. Memo. 2002–210004,* NASA Goddard Space Flight Center, Greenbelt, Maryland, 183–210.

Mueller, J.L., 1984: Effects of water reflectance at 670 nm on Coastal Zone Color Scanner (CZCS) aerosol radiance estimates off the coast of central California. *Ocean Optics VII, Proc. SPIE,* **489,** Bellingham, Washington, 179–186.

Neckel, H., and D. Labs, 1984: The solar radiation between 3,300 and 12,500Å. *Solar Physics,* **90,** 205–258.

O'Reilly, J., S. Maritorena, B. Mitchell, D. Siegel, K. Carder, S. Garver, M. Kahru, and C. McClain, 1998: Ocean color chlorophyll algorithms for SeaWiFS. *J. Geophys. Res.,* **103,** 24,937–24,953.

——, and C. Zetlin, 1998: Seasonal, Horizontal, and Vertical Distribution of Phytoplankton Chlorophyll *a* in the Northeast U.S. Continental Shelf Ecosystem. *NOAA Tech. Report NMFS,* **39,** Fishery Bulletin, 120 pp.

——, S. Maritorena, D.A. Siegel, M.C. O'Brien, D. Toole, B.G. Mitchell, M. Kahru, F.P. Chavez, P. Strutton, G.F. Cota, S.B. Hooker, C.R. McClain, K.L. Carder, F. Müller-Karger, L. Harding, A. Magnuson, D. Phinney, G.F. Moore, J. Aiken, K.R. Arrigo, R. Letelier, and M. Culver, 2000: "Ocean color chlorophyll *a* algorithms for SeaWiFS, OC2, and OC4: Version 4." In: J.E. O'Reilly and 24 Coauthors, SeaWiFS Postlaunch Calibration and Validation Analyses, Part 3. *NASA Tech. Memo. 2000–206892, Vol. 11,* S.B. Hooker and E.R. Firestone, Eds., NASA Goddard Space Flight Center, Greenbelt, Maryland, 9–23.

Palmer, K.F., and D. Williams, 1974: Optical properties of water in the near infrared. *J. Opt. Soc. Amer.,* **66,** 1,107–1,110.

Patt, F.S., 1999: "Assessment of geolocation for SeaWiFS and OCTS using island targets." *Proc. CNES Seminar, In-orbit characterization of optical imaging systems,* Bordeaux, France, November 1999.

——, 2002: Navigation Algorithms for the SeaWiFS Mission. *NASA Tech. Memo. 2002–206892, Vol. 16,* S.B. Hooker and E.R. Firestone, Eds., NASA Goddard Space Flight Center, Greenbelt, Maryland, 17 pp.

——, R.H. Woodward, and W.W. Gregg, 1997: An automated method for navigation assessment for Earth survey sensors using island targets. *Inter. J. Remote Sens.,* **18,** 3,311–3,336.

——, and S. Bilanow, 2001: "Horizon scanner triggering height analysis for OrbView-2." Proc. 2001 Flight Mechanics Symp., *NASA Contractor Rept. 2001–209986,* NASA Goddard Space Flight Center, Greenbelt, Maryland, 559–573.

Podesta, G., 1995: "SeaWiFS Global Fields: What's In a Day?" In: Mueller, J.L., R.S. Fraser, S.F. Biggar, K.J. Thome, P.N. Slater, A.W. Holmes, R.A. Barnes, C.T. Weir, D.A. Siegel, D.W. Menzies, A.F. Michaels, and G. Podesta: Case Studies for SeaWiFS Calibration and Validation, Part 3. *NASA Tech. Memo. 104566, Vol. 27,* S.B. Hooker and E.R. Firestone, Eds., NASA Goddard Space Flight Center, Greenbelt, Maryland, 34–42.

Pope, R.M., and E.S. Fry, 1997: Absorption spectrum (380–700 nm) of pure water. II. Integrating cavity measurements. *Appl. Opt.,* **36,** 8,710–8,723.

Press, W.H., and S.A. Teukolsky, 1992: Fitting straight line data with errors in both coordinates, *Computers in Physics,* **6,** 274–276.

Robinson, W.D., and M. Wang, 2000: "Vicarious calibration of SeaWiFS band 7." In: McClain, C.R., E.J. Ainsworth, R.A. Barnes, R.E. Eplee, Jr., F.S. Patt, W.D. Robinson, M. Wang, and S.W. Bailey, 2000: SeaWiFS Postlaunch Calibration and Validation Analyses, Part 1. *NASA Tech. Memo. 2000–206892, Vol. 9,* S.B. Hooker and E.R. Firestone, Eds., NASA Goddard Space Flight Center, Greenbelt, Maryland, 38–42.

Ruddick, K.G., F. Ovidio, and M. Rijkeboer, 2000: Atmospheric correction of SeaWiFS imagery for turbid coastal and inland waters. *Appl. Opt.,* **39,** 897–912.

Siegel, D.A., M. Wang, S. Maritorena, and W. Robinson, 2000: Atmospheric correction of satellite ocean color imagery: the black pixel assumption. *Appl. Opt.,* **39,** 3,582–3,591.

Sloss, P.W., 1988: Digital Relief of the Surface of the Earth. *Data Announcement 88-MGG-02,* NOAA, National Geophysical Data Center, Boulder, Colorado, 2 pp.

——, 2001: ETOPO2 Database on CD-ROM, NOAA, National Geophysical Data Center, Boulder, Colorado, USA.

Smith, R.C., and W.H. Wilson, 1981: Ship and satellite bio-optical research in the California Bight. *Oceanography from Space,* J.F.R. Gower, Ed., Plenum Press, 281–294.

——, and K.S. Baker, 1981: Optical properties of the clearest natural waters. *Appl. Opt.,* **20,** 177–184.

Siegel, D.A., M. Wang, S. Maritorena, and W. Robinson, 2000: Atmospheric correction of satellite ocean color imagery: the black pixel assumption. *Appl. Opt.,* **39,** 3,582–3,591.

Stumpf, R.P., and M.A. Tyler, 1988: Satellite detection of bloom and pigment distributions in estuaries. *Remote Sens. Environ.,* **24,** 385–404.

——, and J.R. Pennock, 1989: Calibration of a general optical equation for remote sensing of suspended sediment in a moderately turbid estuary. *J. Geophys. Res.,* **94,** 14,363–14,371.

Sydor, M., and R.A. Arnone, 1997: Effect of suspended particulate and dissolved organic matter on remote sensing of coastal and riverine waters. *Appl. Opt.,* **36,** 6,905–6,912.

Tanré, D., M. Herman, P.-Y. Deschamps, and A. De Leffe, 1979: Atmospheric modeling for space measurements of ground reflectances, including bidirectional properties. *Appl. Opt.,* **18,** 3,587–3,594.

Thuillier, G., M. Hersé, P.C. Simon, D. Labs, H. Mandel, D. Gillotay, and T. Foujols, 1998: The visible solar spectral irradiance from 350 to 850 nm as measured by the SOLSPEC spectrometer during the Atlas I mission. *Solar Physics,* **177,** 41–61.

——, ——, ——, ——, ——, ——, and ——, 2003: The solar spectral irradiance from 200 to 2400 nm as measured by the SOLSPEC spectrometer from the Atlas 1-2-3 and EURECA missions. *Solar Physics,* (submitted).

Wang, M., 2003: Correction of artifacts in the SeaWiFS atmospheric correction: Removing the discontinuity in the derived products. *Remote Sens. Environ.,* **84,** 603–611.

——, and S.W. Bailey, 2001: Correction of sun glint contamination on the SeaWiFS ocean and atmospheric products. *Appl. Opt.,* **40,** 4,790–4,798.

——, B.A. Franz, R.A. Barnes, and C.R. McClain, 2001: Effect of spectral bandpass on SeaWiFS-retrieved near-surface optical properties of the ocean. *Appl. Opt.,* **40,** 343–348.

Welschmeyer, N.A., 1994: Fluorometric analysis of chlorophyll *a* in the presence of chlorophyll *b* and phaeopigments. *Limnol. Oceanogr.,* **39,** 1,985–1,992.

Yeh, E-n, M. Darzi, and L. Kumar, 1997: "SeaWiFS Stray Light Correction Algorithm," In: Yeh, E-n, R.A. Barnes, M. Darzi, L. Kumar, E.A. Early, B.C. Johnson, and J.L. Mueller: Case Studies for SeaWiFS Calibration and Validation, Part 4. *NASA Tech. Memo. 104566, Vol. 41,* S.B. Hooker and E.R. Firestone Eds., NASA Goddard Space Flight Center, Greenbelt, Maryland, 24–30.

Young, D.F., P. Minnis, D.R. Doelling, G.G. Gibson, and T. Wong, 1998: Temporal interpolation methods for the clouds and Earth's Radiant Energy System (CERES) experiment. *J. Appl. Meteor.,* **37,** 572–590.

Zege, E.P., A.P. Ivanov, and I.L. Katsev, 1991: *Image Transfer Through a Scattering Medium.* Springer-Verlag, New York, 349 pp.

The SeaWiFS Postlaunch Technical Report Series

Vol. 1

Johnson, B.C., J.B. Fowler, and C.L. Cromer, 1998: The SeaWiFS Transfer Radiometer (SXR). *NASA Tech. Memo. 1998–206892, Vol. 1,* S.B. Hooker and E.R. Firestone, Eds., NASA Goddard Space Flight Center, Greenbelt, Maryland, 58 pp.

Vol. 2

Aiken, J., D.G. Cummings, S.W. Gibb, N.W. Rees, R. Woodd-Walker, E.M.S. Woodward, J. Woolfenden, S.B. Hooker, J-F. Berthon, C.D. Dempsey, D.J. Suggett, P. Wood, C. Donlon, N. González-Benítez, I. Huskin, M. Quevedo, R. Barciela-Fernandez, C. de Vargas, and C. McKee, 1998: AMT-5 Cruise Report. *NASA Tech. Memo. 1998–206892, Vol. 2,* S.B. Hooker and E.R. Firestone, Eds., NASA Goddard Space Flight Center, Greenbelt, Maryland, 113 pp.

Vol. 3

Hooker, S.B., G. Zibordi, G. Lazin, and S. McLean, 1999: The SeaBOARR-98 Field Campaign. *NASA Tech. Memo. 1999–206892, Vol. 3,* S.B. Hooker and E.R. Firestone, Eds., NASA Goddard Space Flight Center, Greenbelt, Maryland, 40 pp.

Vol. 4

Johnson, B.C., E.A. Early, R.E. Eplee, Jr., R.A. Barnes, and R.T. Caffrey, 1999: The 1997 Prelaunch Radiometric Calibration of SeaWiFS. *NASA Tech. Memo. 1999–206892, Vol. 4,* S.B. Hooker and E.R. Firestone, Eds., NASA Goddard Space Flight Center, Greenbelt, Maryland, 51 pp.

Vol. 5

Barnes, R.A., R.E. Eplee, Jr., S.F. Biggar, K.J. Thome, E.F. Zalewski, P.N. Slater, and A.W. Holmes 1999: The SeaWiFS Solar Radiation-Based Calibration and the Transfer-to-Orbit Experiment. *NASA Tech. Memo. 1999–206892, Vol. 5,* S.B. Hooker and E.R. Firestone, Eds., NASA Goddard Space Flight Center, 28 pp.

Vol. 6

Firestone, E.R., and S.B. Hooker, 2000: SeaWiFS Postlaunch Technical Report Series Cumulative Index: Volumes 1–5. *NASA Tech. Memo. 2000–206892, Vol. 6,* S.B. Hooker and E.R. Firestone, Eds., NASA Goddard Space Flight Center, Greenbelt, Maryland, 14 pp.

Vol. 7

Johnson, B.C., H.W. Yoon, S.S. Bruce, P-S. Shaw, A. Thompson, S.B. Hooker, R.E. Eplee, Jr., R.A. Barnes, S. Maritorena, and J.L. Mueller, 1999: The Fifth SeaWiFS Intercalibration Round-Robin Experiment (SIRREX-5), July 1996. *NASA Tech. Memo. 1999–206892, Vol. 7,* S.B. Hooker and E.R. Firestone, Eds., NASA Goddard Space Flight Center, 75 pp.

Vol. 8

Hooker, S.B., and G. Lazin, 2000: The SeaBOARR-99 Field Campaign. *NASA Tech. Memo. 2000–206892, Vol. 8,* S.B. Hooker and E.R. Firestone, Eds., NASA Goddard Space Flight Center, 46 pp.

Vol. 9

McClain, C.R., E.J. Ainsworth, R.A. Barnes, R.E. Eplee, Jr., F.S. Patt, W.D. Robinson, M. Wang, and S.W. Bailey, 2000: SeaWiFS Postlaunch Calibration and Validation Analyses, Part 1. *NASA Tech. Memo. 2000–206892, Vol. 9,* S.B. Hooker and E.R. Firestone, Eds., NASA Goddard Space Flight Center, 82 pp.

Vol. 10

McClain, C.R., R.A. Barnes, R.E. Eplee, Jr., B.A. Franz, N.C. Hsu, F.S. Patt, C.M. Pietras, W.D. Robinson, B.D. Schieber, G.M. Schmidt, M. Wang, S.W. Bailey, and P.J. Werdell, 2000: SeaWiFS Postlaunch Calibration and Validation Analyses, Part 2. *NASA Tech. Memo. 2000–206892, Vol. 10,* S.B. Hooker and E.R. Firestone, Eds., NASA Goddard Space Flight Center, 57 pp.

Vol. 11

O'Reilly, J.E., S. Maritorena, M.C. O'Brien, D.A. Siegel, D. Toole, D. Menzies, R.C. Smith, J.L. Mueller, B.G. Mitchell, M. Kahru, F.P. Chavez, P. Strutton, G.F. Cota, S.B. Hooker, C.R. McClain, K.L. Carder, F. Müller-Karger, L. Harding, A. Magnuson, D. Phinney, G.F. Moore, J. Aiken, K.R. Arrigo, R. Letelier, and M. Culver 2000: SeaWiFS Postlaunch Calibration and Validation Analyses, Part 3. *NASA Tech. Memo. 2000–206892, Vol. 11,* S.B. Hooker and E.R. Firestone, Eds., NASA Goddard Space Flight Center, 49 pp.

Vol. 12

Firestone, E.R., and S.B. Hooker, 2000: SeaWiFS Postlaunch Technical Report Series Cumulative Index: Volumes 1–11. *NASA Tech. Memo. 2000–206892, Vol. 12,* S.B. Hooker and E.R. Firestone, Eds., NASA Goddard Space Flight Center, Greenbelt, Maryland, 24 pp.

Vol. 13

Hooker, S.B., G. Zibordi, J-F. Berthon, S.W. Bailey, and C.M. Pietras, 2000: The SeaWiFS Photometer Revision for Incident Surface Measurement (SeaPRISM) Field Commissioning. *NASA Tech. Memo. 2000–206892, Vol. 13,* S.B. Hooker and E.R. Firestone, Eds., NASA Goddard Space Flight Center, Greenbelt, Maryland, 24 pp.

Vol. 14

Hooker, S.B., H. Claustre, J. Ras, L. Van Heukelem, J-F. Berthon, C. Targa, D. van der Linde, R. Barlow, and H. Sessions, 2000: The First SeaWiFS HPLC Analysis Round-Robin Experiment (SeaHARRE-1). *NASA Tech. Memo. 2000–206892, Vol. 14,* S.B. Hooker and E.R. Firestone, Eds., NASA Goddard Space Flight Center, Greenbelt, Maryland, 42 pp.

Vol. 15

Hooker, S.B., G. Zibordi, J-F. Berthon, D. D'Alimonte, S. Maritorena, S. McLean, and J. Sildam, 2001: Results of the Second SeaWiFS Data Analysis Round Robin, March 2000 (DARR-00). *NASA Tech. Memo. 2001–206892, Vol. 15,* S.B. Hooker and E.R. Firestone, Eds., NASA Goddard Space Flight Center, Greenbelt, Maryland, 71 pp.

Vol. 16

Patt, F.S., 2002: Navigation Algorithms for the SeaWiFS Mission. *NASA Tech. Memo. 2002–206892, Vol. 16,* S.B. er and E.R. Firestone, Eds., NASA Goddard Space Flight Center, Greenbelt, Maryland, 17 pp.

Vol. 17

Hooker, S.B., S. McLean, J. Sherman, M. Small, G. Lazin, G. Zibordi, and J.W. Brown, 2002: The Seventh SeaWiFS Intercalibration Round-Robin Experiment (SIRREX-7), March 1999. *NASA Tech. Memo. 2002–206892, Vol. 17,* S.B. Hooker and E.R. Firestone, Eds., NASA Goddard Space Flight Center, Greenbelt, Maryland, 69 pp.

Vol. 18

Firestone, E.R., and S.B. Hooker, 2003: SeaWiFS Postlaunch Technical Report Series Cumulative Index: Volumes 1–17. *NASA Tech. Memo. 2003–206892, Vol. 18,* S.B. Hooker and E.R. Firestone, Eds., NASA Goddard Space Flight Center, Greenbelt, Maryland, 28 pp.

Vol. 19

Zibordi, G., J-F. Berthon, J.P. Doyle, S. Grossi, D. van der Linde, C. Targa, and L. Alberotanza 2002: Coastal Atmosphere and Sea Time Series (CoASTS), Part 1: A Tower-Based Long-Term Measurement Program. *NASA Tech. Memo. 2002–206892, Vol. 19,* S.B. Hooker and E.R. Firestone, Eds., NASA Goddard Space Flight Center, Greenbelt, Maryland, 29 pp.

Vol. 20

Berthon, J-F., G. Zibordi, J.P. Doyle, S. Grossi, D. van der Linde, and C. Targa, 2002: Coastal Atmosphere and Sea Time Series (CoASTS), Part 2: Data Analysis. *NASA Tech. Memo. 2002–206892, Vol. 20,* S.B. Hooker and E.R. Firestone, Eds., NASA Goddard Space Flight Center, Greenbelt, Maryland, 25 pp.

Vol. 21

Zibordi, G., D. D'Alimonte, D. van der Linde, J-F. Berthon, S.B. Hooker, J.L. Mueller, G. Lazin, and S. McLean, 2002: The Eighth SeaWiFS Intercalibration Round-Robin Experiment (SIRREX-8), September–December 2001. *NASA Tech. Memo. 2002–206892, Vol. 21,* S.B. Hooker and E.R. Firestone, Eds., NASA Goddard Space Flight Center, Greenbelt, Maryland, 39 pp.

Vol. 22

Patt, F.S., R.A. Barnes, R.E. Eplee, Jr., B.A. Franz, W.D. Robinson, G.C. Feldman, S.W. Bailey, J. Gales, P.J. Werdell, M. Wang, R. Frouin, R.P. Stumpf, R.A. Arnone, R.W. Gould, Jr., P.M. Martinolich, V. Ransibrahmanakul, J.E. O'Reilly, and J.A. Yoder, 2003: Algorithm Updates for the Fourth SeaWiFS Data Reprocessing, *NASA Tech. Memo. 2003–206892, Vol. 22,* S.B. Hooker and E.R. Firestone, Eds., NASA Goddard Space Flight Center, Greenbelt, Maryland, 74 pp.

REPORT DOCUMENTATION PAGE

Form Approved
OMNo. 0704-0188

1. AGENCY USE ONLY *(Leave blank)*	2. REPORT DATE	3. REPORT TYPE AND DATES COVERED
	May 2003	Technical Memorandum

4. TITLE AND SUBTITLE
SeaWiFS Postlaunch Technical Report Series
Volume 22: Algorithm Updates for the Fourth SeaWiFS Data Reprocessing

5. FUNDING NUMBERS
970.2

6. AUTHORS F.S. Patt, R.A.Barnes, R.E. Eplee, Jr., B.A. Franz, W.D. Robinson, G.C. Feldman, S.W. Bailey, J. Gales, P.J. Werdell, M. Wang, R. Frouin, R.P. Stumpf, R.A. Arnone, R.W. Gould, Jr., P.M. Martinolich, V. Ransibrahmanakul, J.E. O'Reilly, and J.A. Yoder
Series Editors: Stanford B. Hooker and Elaine R. Firestone

7. PERFORMING ORGANIZATION NAME(S) AND ADDRESS(ES)
Laboratory for Hydrospheric Processes
Goddard Space Flight Center
Greenbelt, Maryland 20771

8. PERFORMING ORGANIZATION REPORT NUMBER
2003-01915-0

9. SPONSORING/MONITORING AGENCY NAME(S) AND ADDRESS(ES)
National Aeronautics and Space Administration
Washington, D.C. 20546–0001

10. SPONSORING/MONITORING AGENCY REPORT NUMBER
TM—2003–206892, Vol. 22

11. SUPPLEMENTARY NOTES E.R. Firestone, F.S. Patt, R.A.Barnes, R.E. Eplee, Jr., B.A. Franz, & W.D. Robinson: SAIC, Beltsville, MD; S.W. Bailey & J. Gales: Futuretech Corp., Greenbelt, MD; M. Wang: University of Maryland, Baltimore County, Baltimore, MD; R. Frouin: Scripps Institution of Oceanography, La Jolla, CA; R.P. Stumpf: NOAA CCMA, Silver Spring, MD; R.A. Arnone, R.W. Gould, Jr., P.M. Martinolich: Naval Research Lab., Stennis, MS; V. Ransibrahmanakul: SPS Technologies, Silver Spring, MD; J.E. O'Reilly: NOAA NMFS, Narragansett, RI; J.A. Yoder: University of Rhode Island, Narragansett, RI.

12a. DISTRIBUTION/AVAILABILITY STATEMENT
Unclassified–Unlimited
Subject Category 48
Report is available from the Center for AeroSpace Information (CASI),
7121 Standard Drive, Hanover, MD 21076–1320; (301)621-0390

12b. DISTRIBUTION CODE

13. ABSTRACT *(Maximum 200 words)*

The efforts to improve the data quality for the Sea-viewing Wide Field-of-view Sensor (SeaWiFS) data products have continued, following the third reprocessing of the global data set in May 2000. Analyses have been ongoing to address all aspects of the processing algorithms, particularly the calibration methodologies, atmospheric correction, and data flagging and masking. All proposed changes were subjected to rigorous testing, evaluation and validation. The results of these activities culminated in the fourth reprocessing, which was completed in July 2002. The algorithm changes, which were implemented for this reprocessing, are described in the chapters of this volume. Chapter 1 presents an overview of the activities leading up to the fourth reprocessing, and summarizes the effects of the changes. Chapter 2 describes the modifications to the on-orbit calibration, specifically the focal plane temperature correction and the temporal dependence. Chapter 3 describes the changes to the vicarious calibration, including the stray light correction to the Marine Optical Buoy (MOBY) data and improved data screening procedures. Chapter 4 describes improvements to the near-infrared (NIR) band correction algorithm. Chapter 5 describes changes to the atmospheric correction and the oceanic property retrieval algorithms, including out-of-band corrections, NIR noise reduction, and handling of unusual conditions. Chapter 6 describes various changes to the flags and masks, to increase the number of valid retrievals, improve the detection of the flag conditions, and add new flags. Chapter 7 describes modifications to the level-1a and level-3 algorithms, to improve the navigation accuracy, correct certain types of spacecraft time anomalies, and correct a binning logic error. Chapter 8 describes the algorithm used to generate the SeaWiFS photosynthetically available radiation (PAR) product. Chapter 9 describes a coupled ocean–atmosphere model, which is used in one of the changes described in Chapter 4. Finally, Chapter 10 describes a comparison of results from the third and fourth reprocessings along the U.S. Northeast coast.

14. SUBJECT TERMS
SeaWiFS, Oceanography, On-Orbit Calibration, Fourth Reprocessing, Vicarious Calibration, NIR Correction, Atmospheric Correction Algorithm, Masks, Flags, Processing Changes, PAR Product, Water-Leaving Radiance, LAC Products, Oceanic Optical Properties

15. NUMBER OF PAGES
74

16. PRICE CODE

17. SECURITY CLASSIFICATION OF REPORT	18. SECURITY CLASSIFICATION OF THIS PAGE	19. SECURITY CLASSIFICATION OF ABSTRACT	20. LIMITATION OF ABSTRACT
Unclassified	Unclassified	Unclassified	Unlimited